Velocity dispersion and wave attenuation of Berea sandstone at different saturations and pressures in seismic frequency band

Qi Huang, De-hua Han, Hemin Yuan, Qianqian, Wei, Min Sun*
Rock Physics Laboratory, University of Houston

Summary

We measured velocities and their attenuation of one Berea sandstone at the different water saturations with fixed differential pressure in seismic frequency band (2-800Hz). Plus, at dry and full water saturation condition, the rock sample was measured at various differential pressures. The measurement results suggest that dispersion is weak and doesn't change with water saturation and differential pressure; whereas, attenuation varies significantly at same measurement conditions. This provides us a good opportunity to investigate the mechanism of dispersion and attenuation, in return, help understand the measured results.

Introduction

Seismic exploration is the principal method using seismic waves to investigate properties of underground petroleum reservoirs. It's based on an important assumption that subsurface structures are elastic. But there is no perfectly elastic media in the Earth. The inelasticity gives rise to velocity dispersion and wave attenuation distorting waveforms, which was observed in seismic, sonic and ultrasonic frequency band.

Dispersion is the variation of seismic wave velocity with frequency, whereas attenuation describes the loss of wave amplitudes with distance. There are several mechanisms that can cause the attenuation including geometric spreading, wave scattering, solid friction and fluid flow. The first two processes are classified as non-intrinsic, while the last two phenomena are considered as intrinsic. No matter in seismic exploration, sonic well-logging or ultrasonic measurement, strain amplitude is less than 10-6, and thus solid friction doesn't occur and fluid flow is the main reason for the intrinsic attenuation (Winkler, Nur, Gladwin, 1979). In past decades, continuous progress in theoretical study of fluid-related dispersion and attenuation in reservoir rocks has been moving forward (Muller et al., 2010). However, all the theories and models haven't received strong support from reliable measured data. We have developed a low frequency (2-800Hz) measurement apparatus to measure the velocity dispersion and wave attenuation. And one Berea sandstone have been measured with it at different water saturations and differential pressures.

Principles of low frequency measurement

The low frequency measurement system can measure the dispersion and attenuation in the seismic frequency band, which consists of mechanical and electronical parts.

In the Fig.1, there is a pressure vessel in which all the mechanical parts are located and a column comprising standard, sample and PZT. Standard is one kind of metal that is repeatedly used because it is elastic and has the fixed Young's modulus with respect to frequency. For example, Aluminum is usually chosen as standard, and its Young's modulus is 69GPa. The sample is covered by a jacket isolating the sample from gas that generates the confining pressure. Two pore pressure lines are connected with the top and bottom of the sample. Thus, the sample can be measured at different confining pressures and pore pressures. On the top of the column there is a piston applying vertical pressure that can make sample, standard and PZT contact tightly. PZT vibrates as a sine function at specified frequency, for example, 2-800Hz. Before measurement, strain gauges are mounted on the surfaces of sample and standard to record strains, including amplitude and phase. Since the force on the whole column is equal everywhere, according to the definition, the Young's modulus of sample can be calculated by

$$E_{sample}(f) = \frac{E_{standard} * \varepsilon_{standard\_vertical}(f)}{\varepsilon_{sample\_vertical}(f)}$$

Where E_{sample} and $\varepsilon_{sample\_vertical}$ are sample's Young's modulus and vertical strain amplitude, $E_{standard}$ and $\varepsilon_{standard\_vertical}$ are standard's Young's modulus and vertical strain amplitude, f is frequency.

Similarly, the Poisson's ratio of sample can be obtained by

$$\nu_{sample}(f) = \frac{\varepsilon_{sample\_horizontal}(f)}{\varepsilon_{sample\_vertical}(f)}$$

Where ν_{sample}, $\varepsilon_{sample\_horizontal}$, $\varepsilon_{sample\_vertical}$ are sample's Poisson's ratio, horizontal strain amplitude and vertical strain amplitude, f is frequency.

And Young's modulus attenuation of sample, namely inverse quality factor, can be calculated by the phase difference between sample's strain and stress (White, 1975),

$$Q_E^{-1}(f) = tan[\theta_{stress}(f) - \theta_{sample\_vertical}(f)]$$

Where Q_E^{-1} is Young's modulus's attenuation, θ_{stress} is stress's phase, $\theta_{sample\_vertical}$ is the sample's vertical strain's phase, f is frequency. According to viscoelastic theory, since the standard is elastic, stress and standard's vertical strain has the same phase. Thus, by replacing the stress's phase with standard's vertical strain's phase in the equation above, the Young's modulus's attenuation of sample is obtained by,

$$Q_E^{-1}(f) = tan[\theta_{standard\_vertical}(f) - \theta_{sample\_vertical}(f)]$$

With three directly measured properties, Poisson's ratio, Young's modulus and its attenuation, other parameters of sample can be calculated, such as P-wave velocity, S-wave Velocity and their attenuation (Batzle, 2006; Spencer, 2016).

As shown in Fig.2, the other important part of low frequency measurement system includes five electronic components, function generator, PZT amplifier, analog amplifier, analog-to-digital converter and computer. At the start, the computer sends a command to function generator with a specified frequency. Then function generator transmits a sine signal to PZT amplifier that drives the PZT actuator to vibrate at the same frequency. The vibrating force generates deformation of sample and standard. Strains on sample and standard are amplified and passed to analog to digital converter. At last, all the strain information, for example, waveform, amplitude and phase of strain, is recorded by data acquisition and processing program.

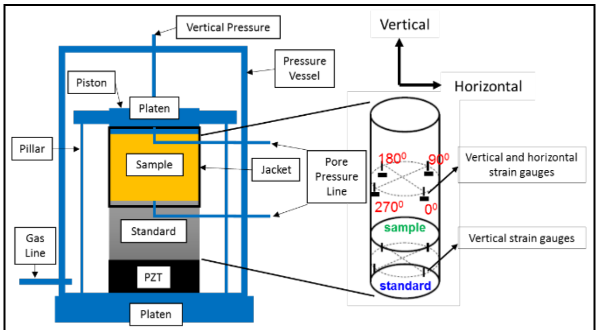

Figure 1: Mechanical part of low frequency measurement system

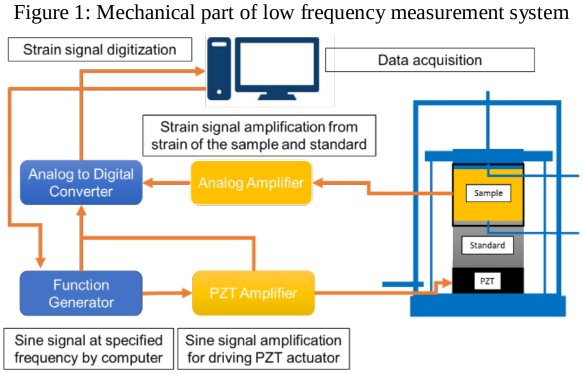

Figure 2: Electronic part of low frequency measurement system

Sample Description

Berea sandstone is a sedimentary rock whose predominant mineral is quartz. It also includes feldspar and extremely small amount of dolomite and clay minerals (Table.1). In the SEM image (Fig.3), the grain size is about 0.12 mm and the pore size is around 0.03 mm.

Table.1. Mineralogy of Berea sandstone sample
unit: weight fraction

Quartz	K-feldspar	Plagioclase	Dolomite	Kaolinite
92.1	3.8	1.3	1.1	0.9

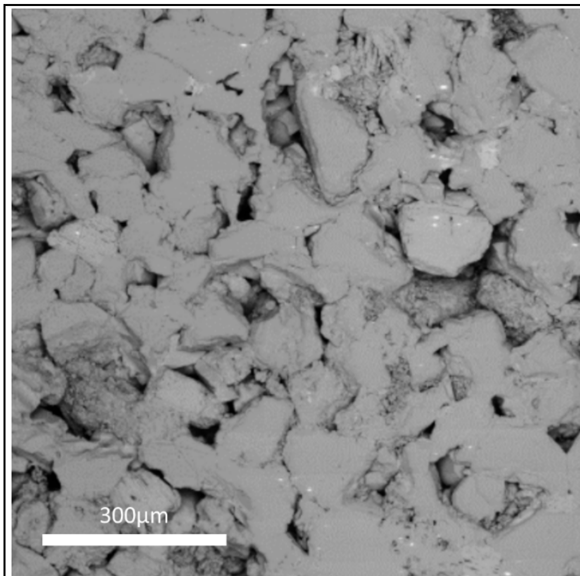

Figure 3: SEM image of Berea sandstone sample

Consequently, the Berea sandstone sample has relatively large porosity and permeability as shown in the Table. 2.

Table.2. Density, porosity and permeability of Berea sandstone sample

Grain Density (g/cc)	Bulk Density (g/cc)	Porosity (%)	Permeability (mD)
2.66	2.05	22.9	662

Measurement results

The Poisson's ratio, Young's modulus and its attenuation of the Berea sandstone sample were measured at different water saturations, from dry to full saturation. And at dry and full water saturation conditions, differential pressures were applied on the sample during measurement.

a) Dry rock measurement
The sample was vacuumed for 48 hours before mounted in the low frequency measurement apparatus and continued to be vacuumed for 2 hours inside pressure vessel to reach dry condition. In the measurement, confining pressure varies from 0 psi to 3000psi.
According to the discussion in the introduction, dry rock has no velocity dispersion and very small attenuation in the

seismic frequency band. This phenomenon was observed from the measured data (Fig.4 and Fig.5). Also, with the increase of confining pressure, we can see the both P-wave and S-wave velocities increase and their attenuation decreases. Particularly, when confining pressure is 3000 psi, the quality factors of P- and S-wave are basically larger than 70, which suggests attenuation is relatively small.

The ultrasonic velocities of the sample were also measured at 1MHz. When compared with the result in seismic frequency band, the ultrasonic velocities are higher (Fig.6). This shows the rock sample are not perfectly elastic, and the velocity dispersion still exists. But the discrepancies between results from two frequency bands reduce as confining pressure increase. Meanwhile, the attenuation decreases (Fig.7). Correspondingly, the dispersion weakens when attenuation becomes smaller. Similarly, when the confining pressure reaches 3000 psi, the velocities in seismic frequency band equals those in ultrasonic frequency band.

b) Partially saturated rock measurement

In this stage of measurement, the water was injected into the sample by ISCO pump that can record the volume of injected water. During the whole process, the differential pressure was kept at 3000psi. When it reached full saturation, pore pressure was 500psi and thus confining pressure was 3500psi.

Due to resonance, both velocities have abnormal points after 500Hz at full water saturation, which are excluded for the following analysis. Because this sample has relatively high permeability, velocities change very little with frequency. Water saturation can change the absolute value of velocities but has no effect on dispersion (Fig.8). When it comes to attenuation, P-wave and S-wave have different behaviors (Fig.9). Although both attenuations increase with water injection, S-wave attenuation has weak frequency dependence, whereas P-wave attenuation are more frequency dependent especially at full water saturation. This suggests P-wave are easier to be affected by fluid than S-wave.

Plus, as the water injected into sample, P-wave velocity decreases before full saturation and increases significantly at full saturation, meanwhile, S-wave velocity keeps dropping (Fig.10). In the saturation process, high frequency components have higher velocity than low frequency components, which indicates the existence of weak dispersion. Unlike velocity dispersion, attenuation of P-wave and S-wave has an obvious leap when sample becomes fully saturated. Plus, P-wave has a more significant increase than S-wave (Fig.11).

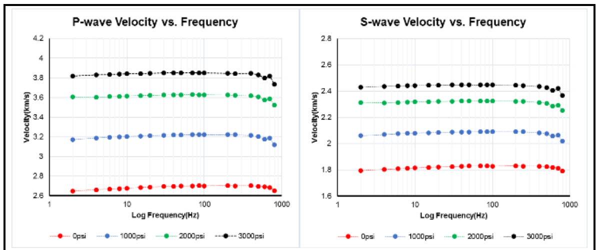

Figure 4: P-wave(left) and S-wave(right) velocity vs. frequency at dry condition

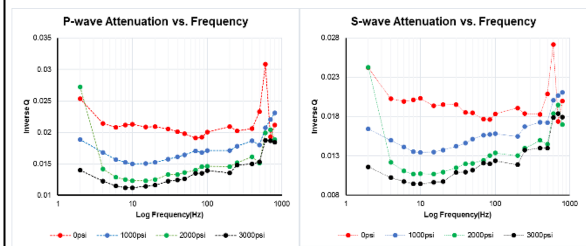

Figure 5: P-wave(left) and S-wave(right) attenuation vs. frequency at dry condition

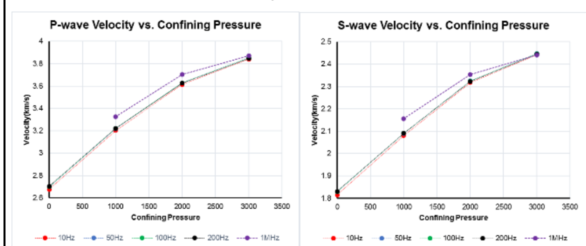

Figure 6: P-wave(left) and S-wave(right) velocity vs. pressure at dry condition

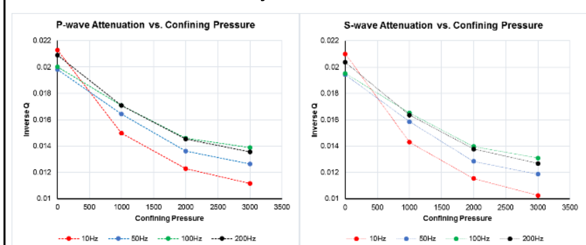

Figure 7: P-wave(left) and S-wave(right) attenuation vs. pressure at dry condition

c) Fully saturated rock measurement

At full saturation, confining pressure was kept at 3000psi, and pore pressure changes from 500psi to 2500psi. Thus, the sample was measured with differential pressure varying from 500psi to 2500psi. Still, the resonance exists at full water saturation, which will be ignored in the following analysis.

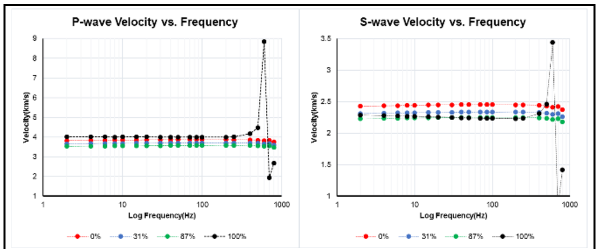

Figure 8: P-wave(left) and S-wave(right) velocity vs. frequency at partial water saturation

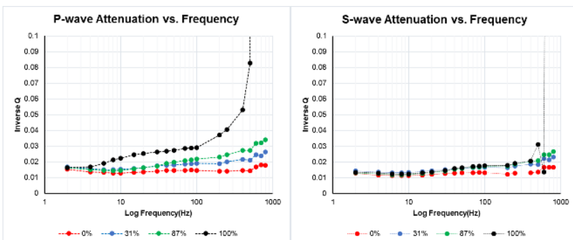

Figure 9: P-wave(left) and S-wave(right) attenuation vs. frequency at partial water saturation

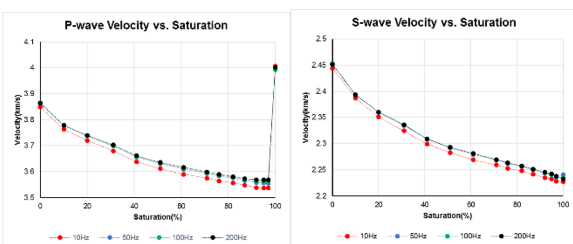

Figure 10: P-wave(left) and S-wave(right) velocity vs. saturation at partial water saturation

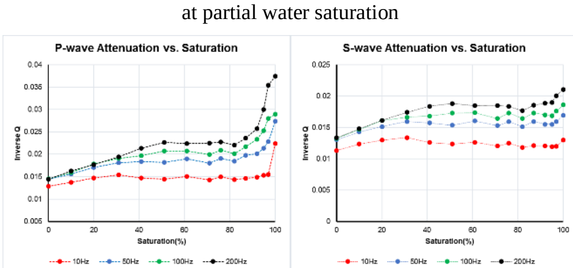

Figure 11: P-wave(left) and S-wave(right) attenuation vs. saturation at partial water saturation

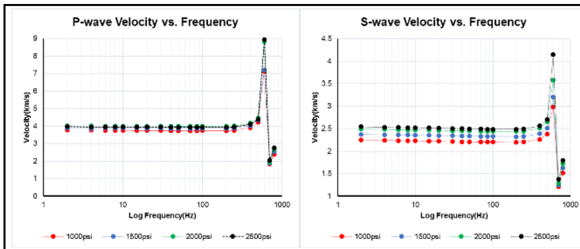

Figure 12: P-wave(left) and S-wave(right) velocity vs. frequency at full water saturation

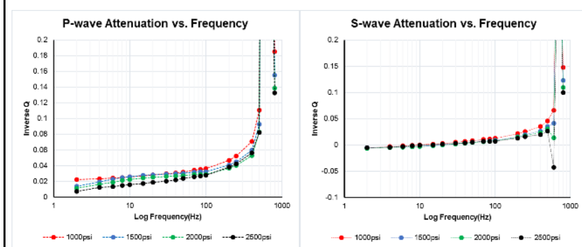

Figure 13: P-wave(left) and S-wave(right) attenuation vs. frequency at full water saturation

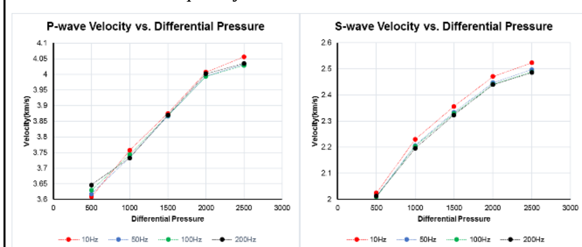

Figure 14: P-wave(left) and S-wave(right) velocity vs. pressure at full water saturation condition

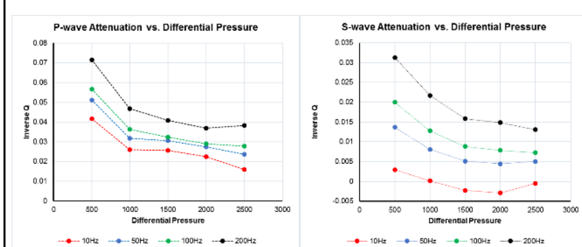

Figure 15: P-wave(left) and S-wave(right) attenuation vs. pressure at dry condition

When sample are full saturated, the velocity has negligible dispersion but attenuation has strong frequency dependence (Fig. 12 and Fig. 13). As differential pressure increases, P-wave and S-wave velocity increase but dispersion still very weak (Fig.14). However, attenuation shows significant pressure dependence and drops drastically with the increase of differential pressure (Fig.15).

Conclusions

First, dry rock is not perfectly elastic medium and thus has dispersion, but it can be ignored in the seismic frequency band. Second, for high-porosity high-permeability rock, water saturation has weak effect on dispersion but strong impact on attenuation. Third, dispersion is not pressure dependent, whereas attenuation highly rely on the differential pressure.

EDITED REFERENCES

Note: This reference list is a copyedited version of the reference list submitted by the author. Reference lists for the 2017 SEG Technical Program Expanded Abstracts have been copyedited so that references provided with the online metadata for each paper will achieve a high degree of linking to cited sources that appear on the Web.

REFERENCES

Batzle, M. L., D. H. Han, and R. Hofmann, 2006, Fluid mobility and frequency - dependent seismic velocity-Direct measurements: Geophysics, **71**, no. 1, N1–N9, http://dx.doi.org/10.1190/1.2159053.

Han, D. H., Q. L. Yao, and M. L. Batzle, 2009, Intrinsic seismic wave attenuation - tight gas sand example: Fluid/DHI consortium annual report.

Hofmann, R., 2006, Frequency dependent elastic and inelastic properties of clastic rocks: Ph.D. dissertation, Colorado School of Mines.

Müller, T. M., B. Gurevich, and M. Lebedev, 2010, Seismic velocity dispersion and wave attenuation resulting from wave-induced flow in porous rocks-A review: Geophysics, **75**, no. 5, 75A147–75A164, http://dx.doi.org/10.1190/1.3463417.

Spencer, J. W., and J. Shine, 2016, Seismic wave attenuation and modulus dispersion in sandstones: Geophysics, **81**, no. 3, D211–D231, http://dx.doi.org/10.1190/geo2015-0342.1

White, J. E., 1975, Computed seismic speeds and attenuation in rocks with partial gas saturation: Geophysics, **40**, 224–232, http://dx.doi.org/10.1190/1.1440520.

Winkler, K., and Nur, A., and Gladwin, M., 1979, Friction and seismic attenuation in rocks: Nature, **277**, 528-531, http://dx.doi.org/10.1038/277528a0.